Oxide characterization of HANA alloys corroded in PWR-simulating condition

Seung Jo Yoo*, Jeong-Yong Park, Byung-Kwon Choi and Yong Hwan Jeong
Advanced Core Materials Lab., Korea Atomic Energy Research Institute,
P.O Box 105 Yuseong, Deajeon 305-600, Korea
**ore78@naver.com*

1. Introduction

HANA alloys exhibited a superior corrosion resistance by optimizing the alloying elements and heat treatment process. The corrosion behavior of the HANA was evaluated with Zircaloy-4 as a reference and the effect of oxide properties on the corrosion behavior was studied. The corrosion testing was performed in 360℃ PWR-simulating loop condition. The oxides formed on HANA alloys were observed by the optical microscopy and the optical transmitted light microscopy to investigate the correlation with the regular transition behavior obtained in the corrosion data. We also measured the nano-hardness on the cross section of oxides to investigate the correlation with the corrosion behavior. The microstructure of the oxides of HANA alloys and reference alloy were connected to the morphological variations form the oxide/metal interface to the oxide/water surface by using transmission electron microscopy. The results of these experiments led to derive the relationship between the oxide characteristics and corrosion behavior of the HANA alloys.

2. Experimental procedure

Three kinds of HANA alloys (HANA-3,4 and 6 alloys whose chemical compositions are Zr-1.5Nb-0.4Sn-0.1Fe-0.1Cu, Zr-1.5Nb-0.4Sn-0.2Fe-0.1Cr and Zr-1.1Nb-0.05Cu, respectively) and Zircaloy-4 alloy were used in this study. The main different thing between the Zricaloy-4 and HANA alloys is that HANA alloys have Nb as a major alloying element but the Zircaloy-4 does not. From the previous researches, Nb has been considered to be very effective for improving the corrosion resistance of the Zr-based alloys among the various alloying elements [1,2].

Corrosion tests were performed in the PWR-simulating loop (Temperature=360℃, Pressure=18.5~18.8MPa, Flow rate = 3~ 4 liter/h, pH 7, Li = 2.2 ppm, B = 650 ppm, O2 < 5 ppb, H < 25 ppb). Corrosion testing specimens, 50 mm in length, were cut from the manufactured tubes and pickled in a solution of H_2O (30 vol.%), HNO_3 (30 vol.%), HCl (30vol.%) and HF (10vol.%). The corrosion resistance was evaluated by measuring the weight gain of the corroded samples after suspending the corrosion test at a periodic term. The maximum exposure for the alloys was 1000 days. In order to understand how the oxide grows and how the microstructure evolves from the oxide/metal interface to the oxide/water surface, it is most profitable to use cross sectional samples. Therefore, in this study, only cross section samples were prepared and used for all the characterization techniques such as OM, TEM and Nano-indentation test. The cross sectional samples which was prepared by the focused ion beam milling were used for transmission electron microscopy.

3. Results and discussion

The corrosion kinetics of the Zircaloy-4 and HANA alloys was compared. Figure 1 shows the weight gain as a function of exposure time collected from corrosion test in the PWR-simulating loop. In the Figure 1, the corrosion rate of HANA alloys was much lower than that of Zircaloy-4. Among the three kinds of HANA alloys, HANA-6 has the highest corrosion resistance. The alloy showing the good corrosion resistance has less transition points during the corrosion test. Zircaloy-4 exhibited 6 transition points whereas HANA-6 showed just one transition point.

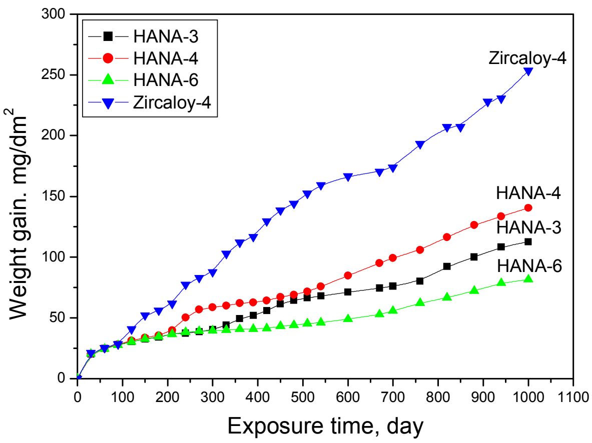

Figure 1. Corrosion behavior of HANA alloys and Zircaloy-4 in PWR-simulating loop.

The general appearance of the cross sectional oxide layers was examined by an optical microscopy. The oxide can be easily distinguished from the metal. It means that the oxide/metal interfaces were discerned clearly and the oxide thickness was able to be measured precisely. From the observation of the cross sectional oxide samples formed after 1000 days corrosion test, it was found that all the alloys have the uniform corrosion with no evidence for the localized corrosion and the roughness of interface was almost the same in all alloys. And the measured oxide thicknesses were in good agreement with the oxide thickness converted from the weight gain data based on the relation that the weight gain of 15 mg/dm^2 = the oxide thickness of 1 μm.

The cross sectional oxide was also examined using the transmitted light optical microscopy. When the thickness of the oxide sample reaches 5-8 μm, the sample becomes transparent to the visible light. In case that the cross sectional oxides samples are observed in the transmitted light mode, various light and dark bands parallel to the oxide/metal interface were observed. While the reflected light images show no contrast, periodic dark bands were observed in transmitted light images for all oxide layers.

The thicknesses of these bands were different depending on the alloy and the observed thicknesses are approximately equal to the thickness of the oxides at the transition. In all oxide, a black layer was formed at the oxide/metal interface. In the oxide on Zircaloy-4, seven bands were counted whereas in HANA-3, 4 and 6 ally oxide, 3,4 and 2 black bands were observed, respectively. The thickness of the layer was higher in Zircaloy-4 when compared to the HANA alloys. For instance, HANA-6 alloy has the thickest oxide layer (3.3 μm) and Zircaloy-4 has the thinnest oxide layer (2.2 μm). It implies that the thickness of the layer is lager in the alloys showing a better corrosion resistance.

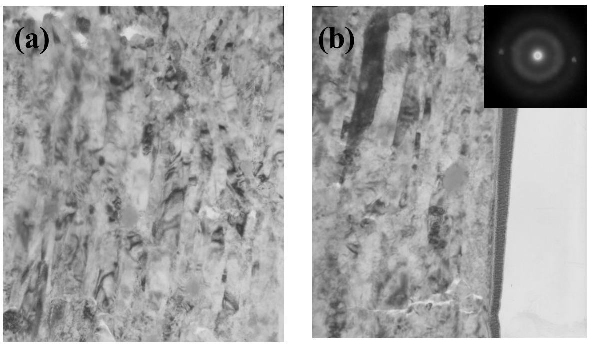

Figure 2. TEM microstructure of (a) the middle section of the oxide and (b) an amorphous precipitate in the oxide of HANA-6 alloy.

By using the Nano-indentation test method, the nano-hardness of the oxide from the oxide/metal interface to the oxide/water surface was measured. HANA-6 alloy showing a better corrosion resistance had lower maximum nano-hardness when compared to the other alloys. The difference between the maximum and minimum nano hardness was lower in the oxide of HANA-6. In the oxide of Zircaloy-4, however, the scattering of nano-hardness value was large, which is attributed to the fact that it the oxide of Zirclaoy-4 was more porous compared to the oxide of HANA-6.

Focused ion beam milled cross sectional samples were examined using transmission electron microscopy. In the oxide, both columnar and small equiaxed grains were observed in all the alloys. However, the grain size of the oxide was different depending on the alloys. HANA alloys have larger columnar and equiaxed grain than Zircaloy-4 alloy. The morphologies of the oxide and incorporated precipitates of HANA-6 was shown in Figure 2. The columnar oxide grains grow in the direction perpendicular to the oxide/metal interface and cracks were observed in the oxide layers. The oxide around the cracks exhibits more equiaxed grains than in the bulk of the oxide.

Second phase particles were incorporated unoxidized into the oxide layer. The metallic second phase particles were observed in the oxide near the oxide/metal interface. After a certain distance from the oxide/metal interface into the oxide layer, both amorphous and oxidized second phase particles were found as shown in Figure 2 (b). In the oxide of Zircaloy-4, the grain decohesion was observed between the small equiaxed and narrow-short columnar grains. Based on the results obtained in this study, the oxide of HANA alloys have a more protective nature against oxygen diffusion as compared to Zircaloy-4.

4. Conclusion

The HANA alloys showed a better corrosion resistance than Zircaloy-4 based on the corrosion test in PWR-simulating loop. The oxides formed on HANA alloys were investigated by various techniques such as OM, TEM and Nano-indentation test. The oxide characterization revealed that the oxide of HANA alloys have a more protective nature against oxygen diffusion as compared to Zircaloy-4.

Acknowledgements

This study was supported by KOSEF and MOST, Korean government, through its National Nuclear Technology Program.

REFERENCES

[1] A.V. Nikulina, J. Nucl. Mater. 238 (1996) 205.
[2] R.J. Comstock, G. Schoenberger, G.P. Sabol, ASTM STP 1295 (1996) 710.